fractal and fractional

MDPI

Article

Flow of a Self-Similar Non-Newtonian Fluid Using Fractal Dimensions

Abdellah Bouchendouka [1], Zine El Abiddine Fellah [1,*], Zakaria Larbi [2], Nicholas O. Ongwen [3], Erick Ogam [1], Mohamed Fellah [4] and Claude Depollier [5]

[1] Aix Marseille Univ, CNRS, Centrale Marseille, LMA UMR 7031, Marseille, 4 Impasse Nikola Tesla CS 40006, CEDEX 13, 13453 Marseille, France
[2] Laboratory of Theoretical and Applied Fluid Mechanics, Physics' Faculty, University of Sciences and Technology Houari Boumediene USTHB, LMFTA BP 32 El Alia, Bab Ezzouar 16111, Algeria
[3] Department of Physics and Materials Science, Maseno University, Maseno 40105, Kenya
[4] Laboratory of Theoretical Physics, Faculty of Physics USTHB, BP 32 El Alia, Bab Ezzouar 16111, Algeria
[5] Laboratoire d'Acoustique de l'Université du Mans (LAUM), UMR 6613, Institut d'Acoustique, CNRS, Le Mans Université, France, Avenue O. Messiaen, CEDEX 09, F-72085 Le Mans, France
* Correspondence: fellah@lma.cnrs-mrs.fr

Abstract: In this paper, the study of the fully developed flow of a self-similar (fractal) power-law fluid is presented. The rheological way of behaving of the fluid is modeled utilizing the Ostwald–de Waele relationship (covering shear-thinning, Newtonian and shear-thickening fluids). A self-similar (fractal) fluid is depicted as a continuum in a noninteger dimensional space. Involving vector calculus for the instance of a noninteger dimensional space, we determine an analytical solution of the Cauchy equation for the instance of a non-Newtonian self-similar fluid flow in a cylindrical pipe. The plot of the velocity profile obtained shows that the rheological behavior of a non-Newtonian power-law fluid is essentially impacted by its self-similar structure. A self-similar shear thinning fluid and a self-similar Newtonian fluid take on a shear-thickening way of behaving, and a self-similar shear-thickening fluid becomes more shear thickening. This approach has many useful applications in industry, for the investigation of blood flow and fractal fluid hydrology.

Keywords: fractal dimensions; power-law fluid; non-Newtonian fluid; self-similar fluid; noninteger dimensional space

Citation: Bouchendouka, A.; Fellah, Z.E.A.; Larbi, Z.; Ongwen, N.O.; Ogam, E.; Fellah, M.; Depollier, C. Flow of a Self-Similar Non-Newtonian Fluid Using Fractal Dimensions. *Fractal Fract.* **2022**, *6*, 582. https://doi.org/10.3390/fractalfract6100582

Academic Editors: Alexander S. Balankin and Didier Samayoa Ochoa

Received: 23 September 2022
Accepted: 7 October 2022
Published: 11 October 2022

1. Introduction

Non-Newtonian fluids appear in a variety of practical applications [1–3]. Their unusual flow patterns are frequently more complicated than those of Newtonian fluids. Numerous studies and observations have shown that for non-Newtonian fluids such as blood, paints, whipped cream and polymeric solutions, the relationship between viscous shear stress and velocity gradient is nonlinear [4–6]. There are a number of empirical or semiempirical formulas that have been developed to accurately measure non-Newtonian viscosity behaviors seen in a variety of disciplines [4–10], namely the well-known power-law model, the Bingham model and the Casson model. In general, both Newtonian and non-Newtonian fluids are thought of as integer-dimensional homogeneous continuums. However, the interior structures of many complex fluids have scale-invariant characteristics that are described by noninteger fractal dimensions [11–14]. An object that possesses scale-invariant features is called a self-similar or fractal object (including fluids), whose fundamental characteristic is that they appear similar under different levels of magnification [11,15]. The mass of a self-similar fluid obeys the power law $M \propto R^D$, where M is the mass of a spherical region of the fluid with radius R, and D is the fractal mass dimension. Fractal fluids include solutions containing a fractal distribution of a solute dissolved in a nonfractal solvent [16], emulsions in which one phase is fractally dispersed in the

other [17], suspensions in which solid particles are fractally distributed in a liquid [18,19] and classical fluids confined in a fractal configuration space [20]. To explain fractal fluids, there exist four basic ways [21,22]: (a) using the methods of "Analysis on fractals" [23–25]; (b) using fractional-differential continuum models [26–30] and also [31–33]; (c) applying fractional-integral continuum models [34,35]; and (d) using the theory of integration and differentiation for a noninteger dimensional space [36–38].

In this paper, we consider the noninteger dimensional space (NIDS) model developed in [39], where the integrations and differentiations are defined for the spaces with noninteger dimensions. Newtonian fractal fluids have been studied by several scientists, including Tarasov [21,40] and Balankin et al. [41]. The study of a fractal non-Newtonian fluid using the noninteger dimensional space model has not yet been considered. In this regard, this study presents a theoretical investigation of the effects of the self-similarity property on the flow of a non-Newtonian fluid through a cylindrical tube. For simplification, the surface of the tube is considered to be smooth. However, for the case of a rough surface, the fractal approach can be used to quantify the irregularities of the tube's inner wall. For instance, a recently published study [42] deals with the influence of the surface roughness on the behavior of a non-Newtonian fluid. However, this is not within the scope of our study. This paper focuses mainly on how the self-similarity property of the fluid affects the flow of a non-Newtonian fluid. The behavior of the non-Newtonian fluid is described using the Ostwald–de Waele model, better known as the power-law model [43]. This approach has a wide range of possible applications in any field that involves a non-Newtonian fluid flow that presents a self-similar structure. For instance, blood is a non-Newtonian fluid that is considered to be self-similar because it contains particles such as proteins, hormones, glucose, etc. Thus, this approach can be used to study blood flow [44,45].

The rest of this paper is organized as follows. In Section 2, we introduce the well-known Ostwald–de Waele model that describes the flow of a non-Newtonian fluid. In Section 3, the noninteger dimensional space operators (gradient and divergence) are presented, and we derive an analytical solution using these operators to describe a self-similar non-Newtonian fluid. A discussion of the results obtained is given in Section 4, and an overall conclusion is presented in Section 5.

2. Laminar Flow of an Incompressible Non-Newtonian Fluid

2.1. The Rheological Behavior of Fluids

The classical Newton's relationship between shear stress and velocity gradient can be expressed as:

$$\overline{\overline{\tau}} = \mu \overline{\overline{\dot{\gamma}}}, \tag{1}$$

where $\overline{\overline{\tau}}$ is the viscous shear stress tensor, μ is the fluid dynamic viscosity and $\overline{\overline{\dot{\gamma}}}$ is the strain rate tensor. The classical Newton's expression of the shear stress can be applied to a particular type of fluids called Newtonian fluids. However, in reality, most fluids do not follow this classical relationship. In fact, different models have been developed to describe the complex behavior of fluids (such as blood, rubber and slurry). Fluids that do not follow the classical Newton's relationship are called non-Newtonian fluids. Several general variations of Equation (1) for various non-Newtonian fluids have been proposed in previous studies. The following power-law model, often known as the Ostwald–de Waele model, is one of the most commonly used formulas:

$$\overline{\overline{\tau}} = K_0 (\overline{\overline{\dot{\gamma}}})^n, \tag{2}$$

where n and K_0 are the power-law index and the consistency index, respectively. For a Newtonian fluid, $n = 1$ and $K_0 = \mu$.

2.2. Momentum Conservation Equation

Let us consider the flow of a non-Newtonian fluid through a cylindrical tube. To model the hydrodynamics of the fluid, we need two equations, conservation of mass and

conservation of momentum or better known as the Cauchy equations, which are written in the following form:

$$\frac{\partial \rho}{\partial t} + \nabla.(\rho \mathbf{v}) = 0, \tag{3}$$

$$\rho \frac{D\mathbf{v}}{Dt} = \rho \mathbf{f} + \nabla.\overline{\overline{\sigma}}, \tag{4}$$

where $\mathbf{v}$ is the velocity field, ρ is the density of the fluid, $\mathbf{f}$ is a vector representing body forces and $\overline{\overline{\sigma}}$ is the stress tensor characterizing the rheological behavior of the fluid.

The stress tensor can be expressed as follows:

$$\overline{\overline{\sigma}} = -p\overline{\overline{I}} + \overline{\overline{\tau}}, \tag{5}$$

where p and $\overline{\overline{I}}$ are the pressure tensor and unit tensor, respectively. $\overline{\overline{\tau}}$ refers to the shear stress tensor.

Considering the case of the fully developed flow of an incompressible non-Newtonian fluid, the mass and momentum conservation Equations (3) and (4) take the following form:

$$\nabla.(\rho \mathbf{v}) = 0 \tag{6}$$

$$-\nabla p + \nabla.\overline{\overline{\tau}} = 0. \tag{7}$$

For a unidirectional flow (along the x direction in Figure 1), the projection of Equation (7) according to the radial coordinate r gives:

$$\nabla_r(-\tau_{xr}\mathbf{e_x}) = \frac{dp}{dx}\mathbf{e_x}, \tag{8}$$

where ∇_r denotes the divergence operator in the radial direction.

Figure 1. Schematic of a cylindrical pipe.

The Poiseuille flow differs from flows with inertia in that the pressure field is independent of the velocity field. Therefore, Equation (8) is written as follows:

$$\frac{1}{r}\frac{d}{dr}(r\tau_{xr}) = \frac{\Delta p}{L}, \tag{9}$$

where $\Delta p > 0$ is the pressure difference along the pipe, and L is the pipe length.

The integration of Equation (9) between $r = 0$ and $r = R$, taking into account the cylindrical symmetry of the pipe at $r = 0$, and using expression (2) for the shear stress τ_{xr}, yields:

$$\frac{dv_x}{dr} = -\left(\frac{\Delta p}{2K_0 L}\right)^{\frac{1}{n}} r^{\frac{1}{n}}. \tag{10}$$

The solution of Equation (10), considering the no-slip condition at the wall, makes it possible to obtain an analytical expression of the velocity field.

$$v_x = v_{max}(n)\left[1 - \left(\frac{r}{R}\right)^{\frac{1+n}{n}}\right], \tag{11}$$

where:

$$v_{max}(n) = \frac{n}{1+n}\left(\frac{\Delta p}{2K_0 L}\right)^{\frac{1}{n}} R^{\frac{n+1}{n}}. \tag{12}$$

The rheological behavior of non-Newtonian fluids is described by Equation (11), a well-known velocity distribution. The constant n is the power-law index, and the fluid is shear thinning (pseudo-plastic) for $0 < n < 1$, Newtonian for $n = 1$ and shear thickening (dilatant) for $n > 1$. Figure 2 illustrates the behavior of these types of fluids.

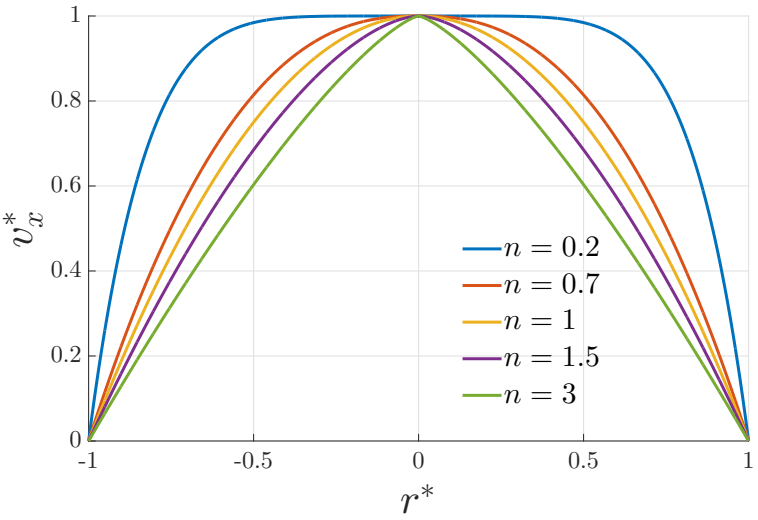

Figure 2. Plot of the velocity profile v_x defined by Equation (11) normalized by V_{max} and $r^* = r/R$.

The non-Newtonian behavior of shear thinning fluids $(0 < n < 1)$ is characterized by a decrease in the viscosity of the fluid under an applied shear strain. The terms "pseudo-plastic behavior" and "shear-thinning behavior" are occasionally used interchangeably [46,47]. It is the most common type of non-Newtonian fluid behavior, and it can be found in a variety of industrial and everyday applications [48]. Although the precise mechanism of shear thinning is unknown, it is widely assumed to be the result of small changes within the fluid, such as the rearrangement of microscale geometries to facilitate shearing. For shear-thickening fluids $(n > 1)$, when shear stress is applied, the viscosity increases. This observable behavior is due to the system crystallizing under stress and acting more like a solid than a solution [49].

3. Laminar Flow of an Incompressible Fractal Non-Newtonian Fluid

Viscous fluids are regarded as being integer-dimensional homogeneous continuums. The internal structures of many complex fluids, on the other hand, have scale-invariant properties, which are characterized by noninteger fractal dimensions. Consider a ball region V_D of radius R of a self-similar fluid; the mass of this ball region is related to its radius by $M \propto R^D$. D is a fractal mass dimension that measures how well the fluid particles fill the region V_D. Generally, for a self-similar fluid, the dimension D takes values less than 3 and for a nonfractal viscous fluid $D = 3$ [40,41]. The boundary S_d of the ball region V_D is characterized by the dimension d, and the relation $d = D - 1$ does not hold in general [21]. Consequently, we define $\alpha_r = D - d$, which is a dimension in the radial direction r. For the case of a noninteger dimensional space, Tarasov proposed a generalization of vector

calculus [39]. The first- and second-order operators such as gradient, divergence, scalar and vector Laplace operators in a noninteger dimensional space (NIDS) are defined. For the sake of simplicity, the scalar and vector fields are assumed to be merely dependent on r (see Refs. [21,39,40] for more details). The divergence and gradient operators in NIDS are written as follows:

$$Div_r^{D,d}\mathbf{u}(r) = \frac{\pi^{(1-\alpha_r)/2}\Gamma((d+\alpha_r)/2)}{\Gamma((d+1)/2)}\left(\frac{1}{r^{\alpha_r-1}}\frac{\partial u_r(r)}{\partial r} + \frac{d}{r^{\alpha_r}}u_r(r)\right), \tag{13}$$

$$Grad_r^{D,d}\phi = \frac{\Gamma(\alpha_r/2)}{\pi^{\alpha_r/2}r^{\alpha_r-1}}\frac{\partial\phi(r)}{\partial r}\mathbf{e}_r, \tag{14}$$

where $\mathbf{u}(r)$ is a vector field and $\phi(r)$ is a scalar field. The NIDS operators (13) and (14) enable us to obtain an equation of motion that describes the flow of a fractal fluid.

Considering the flow of a non-Newtonian fluid with the property of self-similarity, substituting Equations (13) and (14) into Equation (8) we get:

$$Div_r^{D,d}(-\tau_{xr}\mathbf{e_x}) = \frac{dp}{dx}\mathbf{e_x}, \tag{15}$$

where the shear stress τ_{xr} for a fractal fluid is:

$$\tau_{xr} = K_0\left(-\frac{\Gamma(\alpha_r/2)}{\pi^{\alpha_r/2}r^{\alpha_r-1}}\frac{\partial v_x(r)}{\partial r}\right)^n. \tag{16}$$

Applying the divergence and gradient operators for Equation (15), we have the following differential equation:

$$A_n(d_x,\alpha_r)\left[-\frac{n}{r^{(n+1)(\alpha_r-1)}}\frac{d^2v_x}{dr^2}\left(-\frac{dv_x}{dr}\right)^{n-1} + \frac{d_x+n(1-\alpha_r)}{r^{(n+1)\alpha_r-n}}\left(-\frac{dv_x}{dr}\right)^n\right] = \frac{1}{K_0}\frac{\Delta p}{L}. \tag{17}$$

where:

$$A_n = \frac{\Gamma((d_x+\alpha_r)/2)(\Gamma(\alpha_r/2))^n}{\pi^{(\alpha_r(n+1)-1)/2}\Gamma((d_x+1)/2)}. \tag{18}$$

The boundary conditions for Equation (17) are:

$$v_x(0) = V_{max},$$
$$v_x(R) = 0.$$

Considering the new function:

$$Y(r) = \left(-\frac{dv_x(r)}{dr}\right)^n, \tag{19}$$

whose derivative is:

$$Y'(r) = -n\frac{d^2v_x}{dr^2}\left(-\frac{dv_x}{dr}\right)^{n-1}, \tag{20}$$

we can see that $Y(r)$ satisfies the first-order differential equation:

$$rY'(r) + [d_x + n(1-\alpha_r)]Y(r) = Wr^{(n+1)\alpha_r-n}, \tag{21}$$

where:

$$W = \frac{1}{A_n(d_x,\alpha_r)K_0}\frac{\Delta p}{L}. \tag{22}$$

The solution of Equation (21) is:

$$Y(r) = \frac{W}{\alpha_r+d_x}r^{(n+1)\alpha_r-n} + k_1r^{n(\alpha_r-1)-d_x}, \tag{23}$$

where k_1 is a constant. We know that $v_x(0) = V_{max}$, meaning that $v_x(r)$ reaches its maximum value at $r = 0$. Consequently, the derivative of $v_x(r)$ is zero at this value:

$$\frac{dv_x}{dr}(r = 0) = 0. \tag{24}$$

Considering Equations (19) and (24), then $Y(r = 0) = 0$. Notice that the power $n(\alpha_r - 1) - d_x$ in Equation (23) is negative, which leads to an indefined velocity gradient at $r = 0$, implying that $k_1 = 0$. Equation (23) then becomes:

$$Y(r) = \frac{W}{\alpha_r + d_x} r^{(n+1)\alpha_r - n}. \tag{25}$$

Notice that for $Y(r = 0) = 0$, the power $(n + 1)\alpha_r - n$ in expression (25) must be a positive number. Thus, this gives limits to the values permitted for α_r and n. Consequently, we get $\frac{n}{n+1} < \alpha_r \leq 1$.

Considering Equations (19) and (25), we get the following expression for the velocity gradient:

$$\frac{dv_x(r)}{dr} = -(Y(r))^{\frac{1}{n}} = -\left(\frac{W}{\alpha_r + d_x}\right)^{\frac{1}{n}} r^{\alpha_r(1+\frac{1}{n})-1}. \tag{26}$$

After integration, we obtain the following expression for $v_x(r)$:

$$v_x(r) = -\left(\frac{W}{\alpha_r + d_x}\right)^{\frac{1}{n}} \frac{r^{\alpha_r(1+\frac{1}{n})}}{\alpha_r(1 + \frac{1}{n})} + k_2, \tag{27}$$

where k_2 is a constant of integration obtained by the means of the second boundary condition $v_x(R) = 0$:

$$k_2 = \left(\frac{W}{\alpha_r + d_x}\right)^{\frac{1}{n}} \frac{R^{\alpha_r(1+\frac{1}{n})}}{\alpha_r(1 + \frac{1}{n})}. \tag{28}$$

The velocity profile $v_x(r)$ is then given by:

$$v_x(r) = \left(\frac{W}{\alpha_r + d_x}\right)^{\frac{1}{n}} \frac{R^{\alpha_r(1+\frac{1}{n})}}{\alpha_r(1 + \frac{1}{n})} \left[1 - \left(\frac{r}{R}\right)^{\alpha_r(1+\frac{1}{n})}\right]. \tag{29}$$

Using the effective consistency index K_{eff}:

$$K_{eff} = \frac{1}{2}(\alpha_r + d_x)\alpha_r^n A_n(d_x, \alpha_r) K_0, \tag{30}$$

Equation (29) then becomes:

$$v_x(r) = V_{max}\left[1 - \left(\frac{r}{R}\right)^{\alpha_r(\frac{n+1}{n})}\right], \tag{31}$$

where:

$$V_{max} = \frac{n}{n+1}\left(\frac{1}{2K_{eff}}\frac{\Delta p}{L}\right)^{\frac{1}{n}} R^{\alpha_r(\frac{n+1}{n})}. \tag{32}$$

Notice that for $d_x = \alpha_r = 1$, we get the usual velocity distribution of a power-law fluid with $K_{eff} = K_0$ and Equation (31) becomes Equation (11).

4. Discussion

The velocity distribution (31) is proportional to the power $\alpha_r(\frac{n+1}{n})$, meaning that the rheological behavior of a non-Newtonian fluid is heavily dependent on the fractal aspect of the fluid. The fractal dimensions α_r and d_x are a measure of the self-similarity present in the fluid, and the fluid is fractal when $\alpha_r < 1$ and $d_x < 1$. Moreover, Equation (31) shows that, in order to have zero viscous shear effects in the center of the tube, the velocity gradient should equal zero at $r = 0$, which gives a limit to the values permitted for the radial dimension α_r, thus, we get $\frac{n}{n+1} < \alpha_r \leq 1$.

The link between the rheological behavior of a non-Newtonian fluid and its fractal nature can be seen in Figure 3, which plots the effective consistency index K_{eff} defined by Equation (30) normalized by K_0 for different values of n. From Figure 3a, we can see that for a fractal fluid $(\alpha_r < 1)$, K_{eff} increases, the rate of increase, however, being higher for shear-thickening fluids $(n > 1)$. Figure 3b illustrates that for a fractal fluid with $d_x < 1$, K_{eff} decreases in a linear fashion, and the rate of decrease is the same for shear-thinning, Newtonian and shear-thickening fluids. Another interesting result is that the fractal nature of the fluid seems to play a major role in the dynamics of the flow, as it changes completely the rheological behavior of the fluid. Large differences in velocity distributions can be found when different values of fractal dimensions are used. These effects are depicted in Figures 4–6. The behavior of fluids with the property of self-similarity is the same as that of shear-thickening fluids. For a particular value of α_r, shear-thinning fluids $(n < 1)$ and Newtonian fluids $(n = 1)$ behave like shear-thickening fluids (see Figure 4).

In other words, changing the fractal dimension of a fractal non-Newtonian fluid results in a non-Newtonian fluid with different properties. This is because the higher the degree of similarity of the fluid, the thicker this fluid becomes near the walls, which results in a narrower velocity distribution. Not only does the fractal aspect of the fluid affect the shape of the velocity profile, it also has a significant effect on its amplitude (see Figures 5 and 6). However, it is important to note that shear thinning fluids are the most affected by the self-similarity present in the fluid. For values of $\alpha_r < 1$ and $d_x < 1$, the amplitude of the velocity profile increases significantly, especially for shear-thinning fluids.

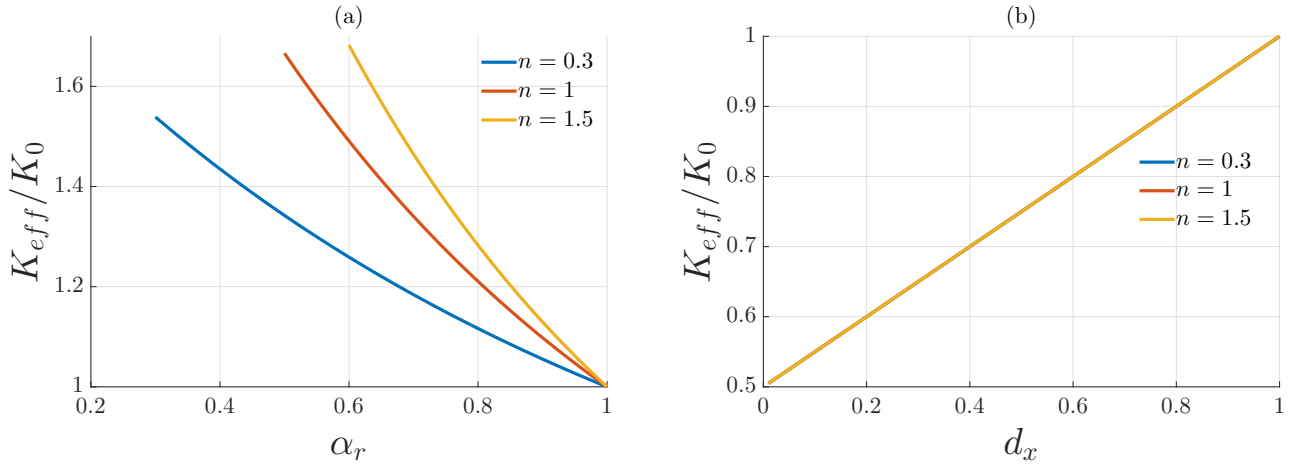

Figure 3. Plot of the effective consistency index of a fractal fluid defined by Equation (30) normalized by K_0 with respect to (**a**) α_r and (**b**) d_x, for different values of n.

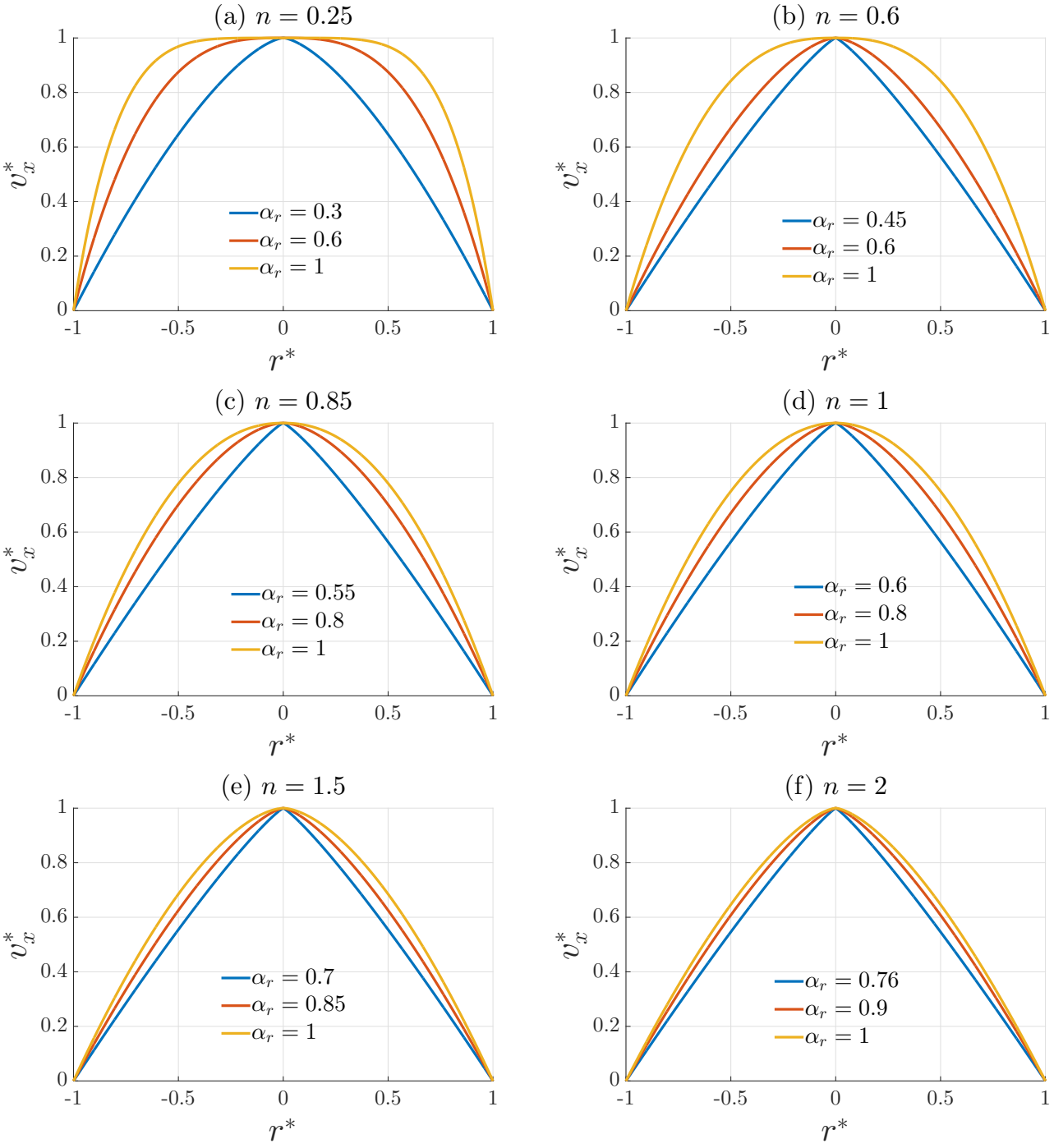

Figure 4. Plot of the normalized velocity profile $v_x^* = v_x / V_{max}$, where v_x is defined by Equation (31), $r^* = r/R$ and the permitted values of α_r in (**a**) $0.2 < \alpha_r \leq 1$, (**b**) $0.375 < \alpha_r \leq 1$, (**c**) $0.46 < \alpha_r \leq 1$, (**d**) $0.5 < \alpha_r \leq 1$, (**e**) $0.6 < \alpha_r \leq 1$ and (**f**) $0.66 < \alpha_r \leq 1$.

It is noteworthy that the radial dimension α_r has the most significant effect on the amplitude of the velocity profile. For $\alpha_r < 1$, the fluid becomes thick near the walls, and because of the conservation of momentum, we see a significant increase in the amplitude of the velocity profile in the center of the tube. By contrast, the dimension d_x only affects the amplitude and not the shape of the velocity profile.

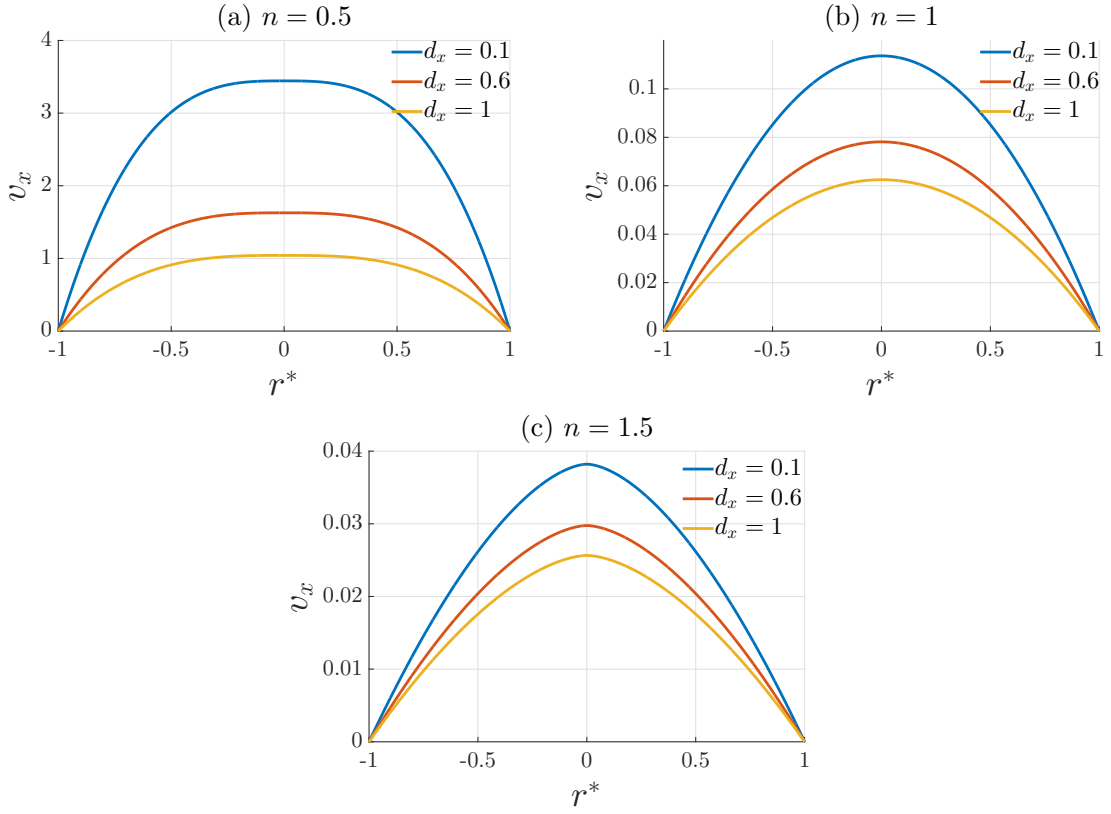

Figure 5. Plot of the profile defined by Equation (31), $r^* = r/R$, $\Delta p/L = 10Pa/m$, $K_0 = 10^{-3}Pa.s^n$ and $\alpha_r = 1$.

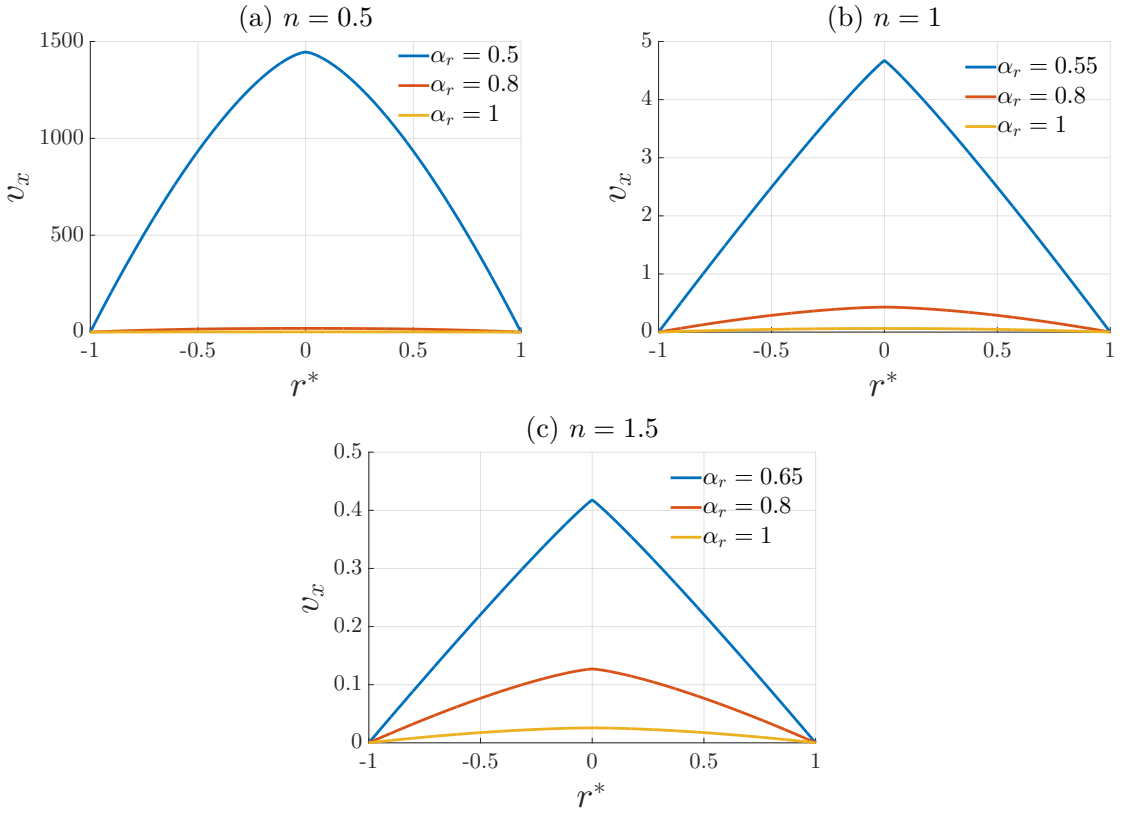

Figure 6. Plot of the profile defined by Equation (31), $r^* = r/R$, $\Delta p/L = 10Pa/m$, $K_0 = 10^{-3}Pa.s^n$, $d_x = 1$ and the values permitted for α_r in (**a**) $0.34 < \alpha_r \leq 1$, (**b**) $0.5 < \alpha_r \leq 1$ and (**c**) $0.6 < \alpha_r \leq 1$.

5. Conclusions

We conducted a theoretical investigation of the fractal nature of a power-law fluid. The fluid was modeled using gradient and divergence operators in NIDS. The equations of motion for an incompressible Stokes flow of a non-Newtonian fractal fluid were derived. Then, a radial velocity distribution describing the behavior of fractal non-Newtonian fluids was obtained. The main parameters affecting the behavior of the flow were the fractal dimensions (α_r,d_x) and the power-law index (n), as the fluid was considered to be a nonfractal Newtonian fluid when $\alpha_r = d_x = n = 1$. We found that for a particular value of α_r, the behavior of self-similar shear-thinning fluids and self-similar Newtonian fluids was similar to that of shear-thickening fluids. The degree of self-similarity affected shear-thinning fluids more significantly than Newtonian and shear-thickening fluids. The approach presented in this paper is applicable to the flow of a power-law fluid exhibiting a fractal structure, for instance, blood flow in the cardiovascular system. As a result, we anticipate that our findings will spur further experimental and theoretical research on the fractal and hydrodynamic aspects of fractal non-Newtonian fluids.

Author Contributions: Writing-Original Draft Preparation, A.B., Z.E.A.F., Z.L., N.O.O., M.F., E.O. and C.D.; Analysis, analytical calculations and processing of results, A.B., Z.E.A F., Z.L., N.O.O., M.F., E.O. and C.D.; Writing-Review & Editing, A.B., Z.E.A.F., Z.L., N.O.O., M.F. and C.D.; Resources, Z.E.A.F., Z.L., N.O.O., M.F., E.O. and C.D. All authors have read and agreed to the published version of the manuscript.

Funding: This research received no external funding.

Data Availability Statement: Not applicable.

Conflicts of Interest: The authors declare no conflict of interest.

References

1. Pandey, V.; Holm, S. Linking the fractional derivative and the lomnitz creep law to non-Newtonian time-varying viscosity. *Phys. Rev. E* **2016**, *94*, 032606. [CrossRef]
2. Bird, R.B.; Dai, G.; Yarusso, B.J. The rheology and flow of viscoplastic materials. *Rev. Chem. Eng.* **1983**, *1*, 1–70. [CrossRef]
3. Mahmood, A.; Parveen, S.; Ara, A.; Khan, N. Exact analytic solutions for the unsteady flow of a non-Newtonian fluid between two cylinders with fractional derivative model. *Commun. Nonlinear Sci. Numer. Simul.* **2009**, *14*, 3309–3319 [CrossRef]
4. Tapadia, P.; Wang, S.Q. Direct visualization of continuous simple shear in non-Newtonian polymeric fluids. *Phys. Rev. Lett.* **2006**, *96*, 016001. [CrossRef]
5. Balmforth, N.J.; Frigaard, I.A.; Ovarlez, G. Yielding to stress: Recent devel- opments in viscoplastic fluid mechanics. *Annu. Rev. Fluid Mech.* **2014**, *46*, 121–146. [CrossRef]
6. Pimenta, T.A.; Campos, A. Friction losses of newtonian and non-Newtonian fluids flowing in laminar regime in a helical coil. *Exp. Therm. And Fluid Sci.* **2012**, *36*, 194–204. [CrossRef]
7. Liao, S.J. On the analytic solution of magnetohydrodynamic flows of non- Newtonian fluids over a stretching sheet. *J. Fluid Mech.* **2003**, *488*, 189–212. [CrossRef]
8. Luikov, A.; Shulman, Z.; Puris, B.; External convective mass transfer in non- Newtonian fluid: Part i. *Int. J. Heat Mass Transf.* **1969**, *12*, 377–391. [CrossRef]
9. Li, B.; Zheng, L.; Zhang, X. Heat transfer in pseudo-plastic non-Newtonian fluids with variable thermal conductivity. *Energy Convers. Manag.* **2011**, *52*, 355–358. [CrossRef]
10. Matsuhisa, S.; Bird, R.B. Analytical and numerical solutions for laminar flow of the non-Newtonian ellis fluid. *AIChE J.* **1965**, *11*, 588–595. [CrossRef]
11. Mandelbrot, B.B. *The Fractal Geometry of Nature*; WH Freeman: New York, NY, USA, 1982; p. 486.
12. Falconer, K.J. *The Geometry of Fractal Sets*; Cambridge University Press: Cambridge, MA, USA, 1986.
13. Feder, J. *Fractals*; Springer Science & Business Media: New York, NY, USA, 2013.
14. Mainardi, F. Fractional calculus. In *Fractals and Fractional Calculus in Continuum Mechanics*; Springer: Berlin/Heidelberg, Germany, 1997; pp. 291–348.
15. Addison, P.S. *Fractals and Chaos: An illustrated Course*; CRC Press: Boca Raton, FL, USA, 1997.
16. Shui, H.; Zhou, H. Viscosity and fractal dimension of coal soluble con- stituents in solution. *Fuel Process. Technol.* **2004**, *85*, 1529–1538. [CrossRef]
17. Hills, B.; Manoj, P.; Destruel, C. Nmr q-space microscopy of concentrated oil-in-water emulsions. *Magn. Reson. Imaging* **2000**, *18*, 319–333. [CrossRef]
18. Shiyan, A. Viscosity for fractal suspensions: Dependence on fractal dimen- sionality. *Phys. Lett. A* **1996**, *220*, 117–119. [CrossRef]

19. Haider, L.; Snabre, P.; Boynard, M. Rheology and ultrasound scattering from aggregated red cell suspensions in shear flow. *Biophys. J.* **2004**, *87*, 2322–2334. [CrossRef]
20. Heinen, M.; Schnyder, S.K.; Brady, J.F.; Löwen, H. Classical liquids in fractal dimension. *Phys. Rev. Lett.* **2015**, *115*, 097801. [CrossRef]
21. Tarasov, V.E. Flow of fractal fluid in pipes: Non-integer dimensional space approach. *Chaos Solitons Fractals* **2014**, *67*, 26–37. [CrossRef]
22. Tarasov, V.E. Anisotropic fractal media by vector calculus in non-integer dimensional space. *J. Math. Phys.* **2014**, *55*, 083510. [CrossRef]
23. Kigami, J. *Analysis on Fractals*; Cambridge University Press: Cambridge, MA, USA, 2001.
24. Strichartz, R.S. Analysis on fractals. *Not. AMS* **1999**, *46*, 1199-1208.
25. Strichartz, R.S. Differential equations on fractals. In *Differential Equations on Fractals*; Princeton University Press: Princeton, NJ, USA, 2018.
26. Carpinteri, A.; Cornetti, P.; Kolwankar, K.M. Calculation of the tensile and flexural strength of disordered materials using fractional calculus. *Chaos Solitons Fractals* **2004**, *21*, 623–632. [CrossRef]
27. Carpinteri, A.; Chiaia, B.; Cornetti, P. A disordered microstructure material model based on fractal geometry and fractional calculus. *ZAMM-J. Appl. Math. Mech. Angew. Math. Und Mech. Appl. Math. Mech.* **2004**, *84*, 128–135. [CrossRef]
28. Yang, X.J.; Srivastava, H.; He, J.H.; Baleanu, D. Cantor-type cylindrical-coordinate method for differential equations with local fractional derivatives. *Phys. Lett. A* **2013**, *377*, 1696–1700. [CrossRef]
29. Yang, X.J.; Baleanu, D.; Tenreiro Machado, J. Systems of navier-stokes equations on cantor sets. *Math. Probl. Eng.* **2013**, *2013*. [CrossRef]
30. Yang, X.J. *Advanced Local Fractional Calculus and Its Applications*; World Science Publisher: Singapore, 2012.
31. Ostoja-Starzewski, M.; Li, J. Fractal materials, beams, and fracture mechanics. *Z. Angew. Math. Phys.* **2009**, *60*, 1194–1205. [CrossRef]
32. Li. J.; Ostoja-Starzewski, M. Fractal solids, product measures and fractional wave equations. *Proc. R. Soc. A Math. Phys. Eng. Sci.* **2009**, *465*, 2521–2536. [CrossRef]
33. Li, J.; Ostoja-Starzewski, M. Micropolar continuum mechanics of fractal media. *Int. J. Eng. Sci.* **2011**, *49*, 1302–1310. [CrossRef]
34. Tarasov, V.E. Continuous medium model for fractal media. *Phys. Lett. A* **2005**, *336*, 167–174. [CrossRef]
35. Tarasov, V.E. Fractional hydrodynamic equations for fractal media. *Ann. Phys.* **2005**, *318*, 286–307. [CrossRef]
36. Collins, J.C. *Renormalization: An Introduction to Renormalization, the Renormalization Group and the Operator-Product Expansion*; Cambridge University Press: Cambridge, MA, USA, 1985.
37. Stillinger, F.H. Axiomatic basis for spaces with noninteger dimension. *J. Math. Phys.* **1977**, *18*, 1224–1234. [CrossRef]
38. Palmer, C.; Starvinou, P.N. Equations of motion in a non-integer dimensional space. *J. Phys. A Math. Gen.* **2004**, *37*, 6987. [CrossRef]
39. Tarasov, V.E. Vector calculus in non-integer dimensional space and its applications to fractal media. *Commun. Nonlinear Sci. And Numerical Simul.* **2015**, *20*, 360–374. [CrossRef]
40. Tarasov, V.E. Poiseuille equation for steady flow of fractal fluid. *Int. J. Mod. Phys. B* **2016**, *30*, 1650128 [CrossRef]
41. Balankin, A.S.; Mena, B.; Susarrey, O.; Samayoa, D. Steady laminar flow of fractal fluids. *Phys. Lett. A* **2017**, *381*, 623–628. [CrossRef]
42. Bouchendouka, A.; Fellah, Z.E.A.; Larbi, Z.; Louna, Z.; Ogam, E.; Fellah, M.; Depollier, C. Fractal analysis of a non-Newtonian fluid flow in a rough-walled pipe. *Materials* **2022**, *15*, 3700. [CrossRef]
43. Shapovalov, V. On the applicability of the ostwald?de waele model in solving applied problems. *J. Eng. Phys. Thermophys.* **2017**, *90*, 1213–1218. [CrossRef]
44. Gabrys, E.; Rybaczuk, M.; Kedzia, A. Blood flow simulation through fractal models of circulatory system. *Chaos Solitons Fractals* **2006**, *27*, 1–7. [CrossRef]
45. Jayalalitha, G.; Deviha, V.S.; Uthayakumar, R. Fractal model for blood flow in cardiovascular system. *Comput. Biol. Med.* **2008**, *38*, 684–693. [CrossRef]
46. Stieger, M. The rheology handbook-for users of rotational and oscillatory rheometers. *Appl. Rheol.* **2002**, *12*, 232–232. [CrossRef]
47. Singh, R.P.; Heldman, D.R. *Introduction to Food Engineering*; Gulf Professional Publishing: Burlington, MA, USA, 2001.
48. Barnes, H.A.; Hutton, J.F.; Walters, K. *An Introduction to Rheology*; Elsevier: Amsterdam, The Netherlands, 1989.
49. Painter, P.C.; Coleman, M.M. *Fundamentals of Polymer Science: An Introductory Text*; Routledge: London, UK, 2019.